Numerical Scrutiny on Friction Factor Characteristics for Protruded Channel under Turbulent Cross-Flow Condition

M. K. Sahu, K. M. Pandey, S. Chatterjee

Abstract*—In the present study, the effect of protrusion pitch, protrusion height, and duct Reynolds number on friction factor characteristics of small rectangular channel with protrusions in cross-flow scheme is analyzed to obtain a suitable configuration of protrusion pattern. Cross-flow is obtained by combining main duct flow (along the direction of length of duct) and nozzle flow which ejects air normal to the protruded bottom wall for the enhancement of heat transfer rate. Finite volume method is used to solve conservation of mass, momentum, and energy equations along with k-ω turbulence model for the analysis of hydraulic performance of protruded channel. Reynolds number from 8360 to 33950 for duct flow and 5120 for nozzle flow are considered with air as working fluid. It is predicted that the friction factor is increased with the increase in protrusion pitch.

***Index Terms*— Channel, Cross flow, Friction factor, Protrusion.**

I. INTRODUCTION

Nowadays, different passive and active heat transfer enhancements techniques are used such as fin heat transfer, forced convection heat transfer, jet impingement cooling, ribs, dimples, grooves, vortex generator on heated surface, etc. But, heat transfer enhancement techniques simultaneously increase the pressure drop. Therefore, study of flow friction characteristics is necessary along with heat transfer analysis.

The flow friction and heat transfer analysis have been applied in different industrial applications such as in solar air heater, gas turbine, electronic cooling, refrigeration, and compact heat exchangers [1-7].Sahu*et al.* [8] investigated thermo-hydraulic performance of rectangular channel with right angle triangular protrusions under cross flow condition and found increase in pressure drop with increase in protrusion height. Barik *et al.*[9] studied numerically for hydraulic and thermal performance in the small rectangular channel with triangular, rectangular, and trapezoidal protruded bottom surface with cross-flow of jet. They found increase in pressure drop and pumping power due to protrusions.

From the literature survey, it is observed that most of the researches are focused on heat transfer and friction factor analysis on rough surface without considering cross flow effect. Some investigations are considered the cross flow cooling of the protruded surface channel without considering the effect of protrusion pitch and height into account. In the present study, the effect of protrusion pitch, protrusion height, and duct Reynolds number on friction factor characteristics of channel with protrusions in cross-flow condition is analyzed. The suitable configuration of protrusion pattern is directly influenced the pumping power requirement of electronic cooling device.

II. PHYSICAL DESCRIPTION AND GRID GENERATION

The computational domain of channel having protrusions with different boundary conditions is presented in Fig. 1.The rectangular duct having total length of 670 mm, width 30 mm and height of 23 mm is considered. The total length of duct is divided into three parts namely inlet extended region, test section, and outlet extended region. The inlet extended region of length 260 mm is considered to achieve fully developed and uniform velocity of air flow through the test section. The length of test section is 150 mm which is heated from the bottom protruded wall with constant temperature T_w. The outlet section is extended to 260 mm length so that back flow and recirculation can be avoided at the exit. At the duct inlet, air is flowing with velocity of u_{in} and ambient temperature of T_a. At the centerof top wall (opposite to bottom heated test section), square shape nozzle of dimension 5 mm × 5 mm impinges air normal to the protruded heated surface with velocity v_{in} and temperature T_a. Therefore, duct flow and nozzle flow increases the turbulence and resulting in enhancement in heat transfer rate. In the heated surface, different heights and pitches of protrusions of isosceles triangular shape are considered for this analysis. Arrangements of isosceles triangular protrusion with different heights and pitches are presented in Fig.2. The height of protrusions (e) is 3 mm, 5 mm, and 7 mm are considered. The base length of each isosceles protrusion is 8mm. The protrusion pitches (p) of 20 mm, 25 mm, and 30 mm are taken. Reynolds number of duct flow is varied from 8360 to 33950 with constant Reynolds number of 5120 in nozzle flow.

Revised Manuscript Received on April 12, 2019.

M. K. Sahu, Department of Mechanical Engineering, National Institute of Technology, Silchar, Assam-788010, India. (E-mail: manojsahu123@gmail.com)

K. M. Pandey, Department of Mechanical Engineering, National Institute of Technology, Silchar, Assam-788010, India. (E-mail: kmpandey2001@yahoo.com)

S. Chatterjee, Department of Mechanical Engineering, Cooch Behar Government Engineering College, Cooch Behar, West Bengal-736170, India. (E-mail: sushovan.chatterjee@gmail.com)

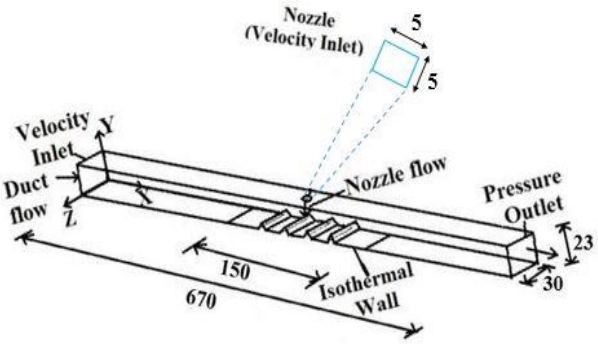

Fig.1. Computational domain with Boundary conditions (All dimensions are in mm).

The grid arrangement of the computational domain with expanded view of triangular protruded channel is shown in Fig.3. Grids are generated using ANSYS 14.0 meshing [10]. The tetra and hexa dominant mesh are generated in the test section. The inlet and exit extended region is meshed with hexahedral mesh due to smooth bottom wall. Inflation layer is added on inside wall of protruded channel with suitable first layer thickness to have y^+ value close to one, so that flow physics of near wall region is captured. The test section is made of dense mesh to predict accurately Nusselt number and friction factor, however, inlet and outlet extended region is made of less dense mesh so that number of cells is minimized without affecting the solution.

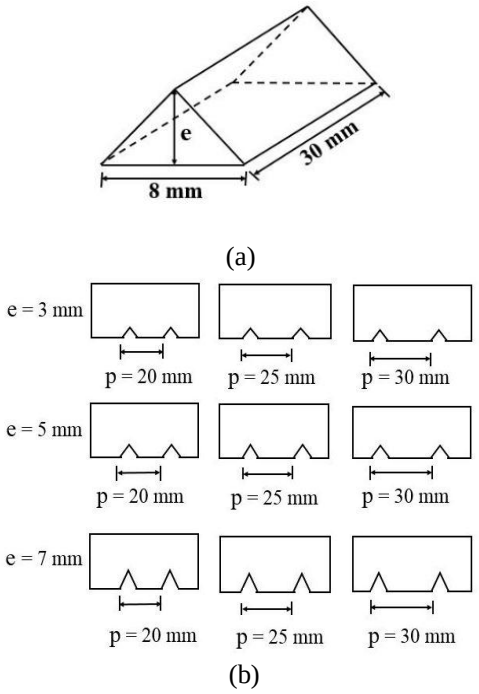

Fig.2. (a) Dimension of Triangular protrusion (b) Configuration of protrusion pattern.

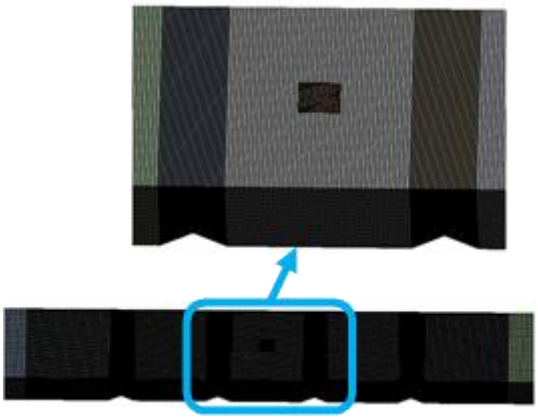

Fig.3. Grid arrangement with expanded view of triangularprotruded channel

III. NUMERICAL METHODOLOGY

For turbulent flows, Reynolds time averaging of governing equations are as follows [9].

Continuity equation:

$$\frac{\partial U_i}{\partial x_i} = 0 \tag{1}$$

Momentum equation:

$$\rho U_j \frac{\partial U_i}{\partial x_j} = -\frac{\partial P}{\partial x_i} + \frac{\partial}{\partial x_j}\left(2\mu S_{ij} - \rho \overline{u_i' u_j'}\right) \tag{2}$$

Energy equation: $$\rho U_j \frac{\partial T}{\partial x_j} = \frac{\partial}{\partial x_j}\left(\frac{\lambda}{c_p}\frac{\partial T}{\partial x_j} - \rho \overline{T' u_j}\right) \tag{3}$$

where, S_{ij} is mean strain rate

$$S_{ij} = \frac{1}{2}\left(\frac{\partial U_i}{\partial x_j} + \frac{\partial U_j}{\partial x_i}\right) \tag{4}$$

where $\left(-\rho \overline{u_i' u_j'}\right)$ denotes Reynolds stress

$$-\rho \overline{u_i' u_j'} = 2\mu_t S_{ij} - \frac{2}{3}\rho k \delta_{ij} \tag{5}$$

Turbulent heat flux is

$$-\rho \overline{u_i' T'} = \frac{\mu_t}{\mathrm{Pr}_t}\frac{\partial \overline{T}}{\partial x_i} \tag{6}$$

where Pr_t is turbulent Prandtl number

Shear stress transport (SST) based k-ω turbulence model introduced by Menter [11] is used for modeling turbulence quantities.For jet impingement cooling; SST k-ω turbulence model is suggested by various researchers [12-14]

Governing equation for turbulence kinetic energy (k) is given as

$$\frac{\partial}{\partial x_i}(\rho k u_i) = \frac{\partial}{\partial x_j}\left[\left(\mu + \frac{\mu_t}{\sigma_k}\right)\frac{\partial k}{\partial x_j}\right] + \min\left(P_k, 10\rho\beta^* k\omega\right) - \rho\beta^* k\omega \tag{7}$$

Equation for Specific dissipation rate (ω) is

$$\frac{\partial}{\partial x_i}(\rho\omega u_i)=\frac{\partial}{\partial x_j}\left[\left(\mu+\frac{\mu_t}{\sigma_k}\right)\frac{\partial\omega}{\partial x_j}\right]+\frac{\alpha\omega}{\kappa}P_k-\rho\beta\omega^2 2(1-F_1)\frac{\rho\sigma_{\omega,2}}{\omega}\frac{\partial k}{\partial x_j}\frac{\partial\omega}{\partial x_j} \quad (8)$$

Turbulent viscosity is formulated as

$$\mu_t=\rho\frac{k}{\omega}\frac{1}{\max\left(\frac{1}{\alpha^*},\frac{SF_2}{a_1\omega}\right)} \quad (9)$$

where S is the mean rate of strain tensor.Coefficients α* is

$$\alpha^*=\alpha_\infty^*\left(\frac{\alpha_0^*+\frac{\mathrm{Re}_t}{R_k}}{1+\frac{\mathrm{Re}_t}{R_k}}\right) \quad (10)$$

where blending functions, $F_1=\tanh\left(\varphi_1^4\right)$ and $F_2=\tanh\left(\varphi_2^2\right)$ .Here, ϕ_1 and ϕ_2 are given

$$\varphi_1=\min\left[\max\left(\frac{\sqrt{k}/0.09\omega y,}{500\mu/\rho y^2\omega}\right),4\rho k/\sigma_{\omega,2}D_\omega^+y^2\right],$$

$$\varphi_2=\max\left[(2\sqrt{k}/0.09\omega y),(500\mu/\rho y^2\omega)\right]$$

Cross-diffusion term, D_ω^+ is

$$D_\omega^+=\max\left[2\rho/\sigma_{\omega,2}\ \omega\partial k/\partial x_j\ \partial\omega/\partial x_j,\ 10^{-10}\right]$$

Turbulence kinetic energy production is

$$P_k=-\rho\overline{u_i'u_j'}\frac{\partial u_i}{\partial x_i} \quad (11)$$

As, we assume flow to be incompressible, β* is equal to βi*, which is given as

$$\beta_i^*=\beta_\infty^*\left(\frac{4/15+\left(\mathrm{Re}_t/R_\beta\right)^4}{1+\left(\mathrm{Re}_t/R_\beta\right)^4}\right) \quad (12)$$

SST k-ω turbulence model has some model constants which are given as $\alpha_\infty^*=1$, $\beta_\infty^*=0.09$, $\beta_i=0.072$, $\sigma_{k,1}=1.176$, $\sigma_{\omega,1}=2$, $\sigma_{k,2}=1$, $\sigma_{\omega,2}=1.168$, $R_\beta=8$, $R_k=6$

$a_1=0.31$

Different boundary conditions on Computational domain are presented in Fig. 1

Boundary conditions in mathematical form can be written as:

Duct entry: $u=u_{in}$ and $T=T_{in}=300$ K (13)

Nozzle entry: $v=-v_{in}$ and $T=T_{in}=300$ K (14)

Duct outlet: $P=P_a$ and $T=T_a$ (15)

Heated surface: $u_j=0$ and $T=T_w=353$ K (16)

Insulated walls: $u_j=0$ and $\frac{\partial T}{\partial x}=\frac{\partial T}{\partial y}=\frac{\partial T}{\partial z}=0$ (17)

where u_j is velocity component in x, y, and z direction

For mean velocity, the law of wall is written as

$$\frac{U_p k_p^{1/2}c_\mu^{1/4}}{\tau_\omega/\rho}=\frac{1}{\kappa}\ln\left(Ey^*\right) \quad (18)$$

$$\text{where, } y^*=\frac{\rho\kappa_p^{1/2}c_\mu^{1/4}y_p}{\mu} \quad (19)$$

where value of Empirical Constant E is 9.793, von Karman constant κ has value of 0.4187. Turbulence intensity at the duct and at the nozzle inlet can be calculated as

$$I=0.16\left(\mathrm{Re}\right)^{-1/8} \quad (20)$$

Equations of continuity, momentum, and electricity together with delivery equation for turbulence kinetic power (good enough) and unique dissipation price (ω) are discretized. Simple scheme [15] has been carried out for pressure-speed coupling. The algebraic equations are solved for go along with the glide area by way of the usage of applying finite quantity based totally code Ansys Fluent 14.Zero [10]. The performance parameters are calculated

Reynolds number at duct inlet is

$$\mathrm{Re}_d=\frac{\rho u_{in}D_{h,duct}}{\mu} \quad (21)$$

Similarly, Reynolds number of nozzle can be determined from hydraulic diameter and inlet velocity of nozzle.

Friction factor,

$$f=\left(\Delta P\Big/\left(\frac{1}{2}\rho u^2\right)\right)\frac{D_{h,duct}}{L} \quad (22)$$

where ΔP is pressure drop.

IV. RESULTS AND DISCUSSIONS

The rectangular channel with distensions having top 5 mm and pitch 25 mm at course and gush Reynolds huge style of 17180 and 5120, independently, is thought about for network fair examination. 5 units of grid term having 338358, 375902, 476960, 538800, and 611070 cells are considered. The astoundingly minor deviation (0.02 %) in Nusselt wide range is done while proportion of cross section cells will advancement from 538800 to 611070. In this way, 538800 cells are taken as structure fair-minded to shop computational resource with reasonable exactness.

The transcendent computational fluid components (CFD) ask about is showed up with Sleicher and Rouse [16] and associations. It is arranged that surrender last result of numerical methodology reasonably simultaneousness with Sleicher and Rouse [16] association and therefore it demonstrates the reliability of numerical arrangement for further examination for grinding segment appraisal.

From Fig.4, it's far picked that the disintegration segment decreases with the extension in Reynolds sum. It's far a direct result of disguise of thick sub-layer at higher Reynolds wide range. It is moreover observed that the disintegration segment is extra for all courses of action of enlarged direct in evaluation to basic channel. It's far a direct result of impediment of float in stuck channel and in this way, strain drop and scouring inconvenience is connected for enlarged channel.

It's miles found that crushing burden is extra in greater pitch of projection. It's miles in light of free shear layer reattachment and dissemination inside the openings among lumps wherever pitch. Along these lines, the strain drop and scouring issue is expanded at greater pitch of lump.

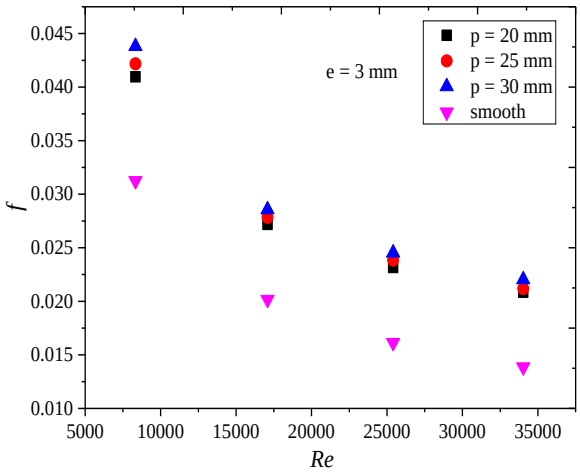

(a) Height of protrusions e = 3 mm

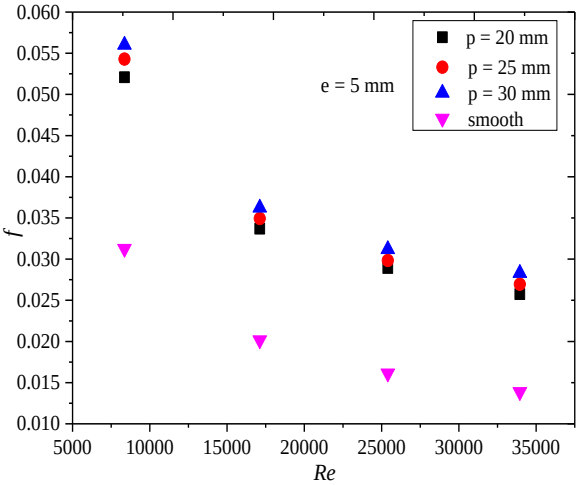

(b) Height of protrusions e = 5mm

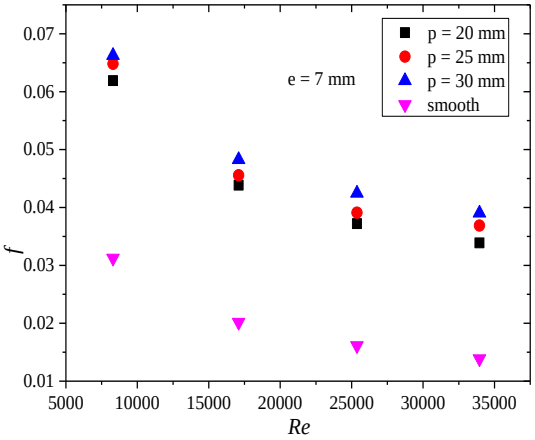

(c)Height of protrusions e = 7 mm

Fig. 4. Friction factor Versus Reynolds number for number for different height of protrusions.

From Fig.4 (a)-(c), for particular protrusion pitch and duct Reynolds number, it is noticed that, the friction factor is increased with the increase in protrusion height. It is due to reduction in cross section area for flow at protrusion region. Therefore, the fluid molecules are accelerated after passing through protrusion region which increases the pressure drop. Thus, friction factor is increased with the increase in protrusion height.

V. CONCLUSIONS

Flow friction characteristics are numerically analyzed for rectangular channel with protrusions of triangular shape having different heights and pitches on the heated wall (bottom) of test section under cross flow condition. The major findings from this studies are given below:

Friction factor value decreases with increase in Reynolds number for the protruded channel. The friction factor of protruded channel is noticed to be more than the smooth channel.

Friction factor value is more at larger pitch for all the considered protrusions pattern. The value of friction factor is higher for larger protrusion height.

ACKNOWLEDGMENT

The makers want to need to provide gratitude to the branch of Mechanical Engineering, NIT Silchar, Assam, India for giving Computational Fluid Dynamics lab offices and besides perceive TEQIP III for givingeconomic assist to complete the examination work.

VI. REFERENCES

1. A. S. Yadav, and J. L. Bhagoria, A Numerical examinations of rectangular portioned transverse rib roughened daylight based air hotter. Generally speaking magazine of Thermal Sciences vol.Seventy nine, pp.111–31, 2014.
2. J.L. Bhagoria, J.S. Saini, and S.C. Solanki, warmth trade coefficient and scouring issue associations for square daylight based air hotter pipe having transverse wedge-framed rib brutality on the protect plate, Renewable power vol. 25, pp.341–369, 2002.

3. A. S. Yadav, and J.L. Bhagoria, A CFD (computational fluid components) based absolutely warmth switch and fluid buoy appraisal of a sun based air radiator gave round transverse twine rib cruelty on the shield plate, quality, vol.Fifty five, pp. 1127-1142, 2013.
4. V. B. Gawande, A. S. Dhoble, D. B. Zodpe, and S. Chamoli, Experimental and CFD-based warm execution estimate of sun air radiator furnished with right-perspective triangular rib as built cruelty, J Braz. Soc. Mech. Sci. Eng. Vol.38, pp. 551–579, 2016.
5. R. Kumar, V. Geol, and A. Kumar, A parametric examination of the 2d model of sun air hotter with round rib repulsiveness the usage of CFD, journal of Mechanical age and development vol.31 (2), pp.959-964, 2017.
6. L. Wang, S. Wang, F. Wen, X. Zhou, and Z. Wang, consequences of steady wavy ribs on warmth trade and cooling air acknowledge conditions for what they are in a square single-skip channel of turbine bleeding edge, overall magazine of warmth and Mass trade, vol. 121, pp.514–533, 2018.
7. L. T. Yeh, survey of warmth switch age in mechanized contraption, mag of virtual Packaging, vol. 117(four), pp. 333-339, 1995.
8. M. Attractive. Sahu, OK. M. Pandey, S. Chatterjee, Numerical examination of warm water driven general execution of channel with lumps by the use of rough stream float fly", AIP show methods vol. 1966, 020021 (2018)
9. A. Adequate. Barik, A. Mukherjee, and P. Patro, warm temperature change improvement from a little rectangular station with tremendous surface lumps with the advantage of a furious go together with the buoy fly, all inclusive magazine of Thermal Sciences vol.98, pp.32–forty one, 2015.
10. ANSYS Fluent 14.Zero thought manual, ANSYS, Inc, Canonsburg, PA 15317, 2011.
11. F.R. Menter, two-condition twirl consistency unevenness models for planning packs. American Institute of Aeronautics and Astronautics magazine vol.32, pp.1598-1605, 1994.
12. A. Okay. Shukla, and A. Dewan, Convective warm temperature switch Enhancement the use of Slot Jet Impingement on a detached Rib surface. Journal of finished Fluid Mechanics vol.10(6), pp.1615-1627, 2017.
13. M.A.R. Sharif, and k.Good enough. Mothe, assessment of aggravation models inside the desire for warmth trade as a result of opening plane impingement on plane and bended surfaces. Numerical warmness switch. Part B, vol.Fifty five, pp.273-294, 2009.
14. N. Zuckerman, and N. Lior, Impingement warmth switch: associations and numerical illustrating, ASME, journal of warmth switch vol.127, pp.544-552, 2005.
15. S.V. Patankar, Numerical warmth switch and Fluid take the easy way out, Hemisphere Publishing office, new york, 1980
16. C.A. Sleicher, and M.W. Invigorate, A helpful association for warmth trade to reliable and variable impacts fluids in savage pipe coast, worldwide magazine of warmth Mass switch vol.18, pp.677-683, 1975.